

Detection of Finger-Knuckle-Print Images: A Review

Ekta Tamrakar¹, Mina Mishra²

Dept. of Electronics and Telecommunication Engineering, BIT, Durg, C.G, India¹

Dept. of Electronics and Telecommunication Engineering, CCET, Bhilai, C.G, India²

Email Id: ¹ektatamrakar@gmail.com, ²minamishraetc@gmail.com

Abstract

Automated security is one of the major concerns of modern times. Secure and reliable authentication systems are in great demand. A biometric trait like Finger Knuckle Print (FKP) of a person is unique and secure. In the recent years, hand based biometrics is extensively used for personal recognition. Finger Knuckle has unique bending and makes a distinctive biometric identifier. Automatic Knuckle print recognition systems are based on local ridge features known as Minutiae. To select the minutiae points properly and rejecting unwanted ones is very important. The Proposed system shows various methods to implement various aspects of Recognition. There are various filters, Wavelet Transform Methods to implement the Authentication.

Keywords: *Finger Knuckle Print (FKP), Recognition, Minutiae, Authentication.*

1. Introduction:

Swati M R et al. [1] developed Biometric authentication is a process of identifying a person by his/her characteristics or traits. The characteristics/traits which are used to describe a person can be categorized into two groups. Namely physiological characteristics and behavioural characteristics. The behavioural characteristics refer to the behaviour of a person which includes typing rhythm, voice, gait etc and the Physiological characteristic refers to the feature or shape of human body which includes finger print, iris, ear pattern, DNA, palm print, face etc. The recent study shows that prominence of the dorsal aspect of a joint of a finger which is also known as finger knuckle area which consists of highly rich lines and creases are unique and distinct for every individual.

C Hegde et al. [2] suggested the user acceptance for the outer finger surface imaging can be very high as, unlike popular fingerprints, there is no stigma of criminal investigation associated with finger knuckle surface imaging. The peg-free imaging of the finger knuckle surface is highly convenient to users and offers very high potential for reliable personal identification and authentication. The appearance based approach investigated. For the finger knuckle identification cannot exploit line based features and therefore achieves moderate performance. The finger knuckle surface is highly rich in lines and creases, which are rather curved but highly unique for individuals.

2. Steps

2.1 Pre-processing

Swati M Ret al. [1] projected the image present in the PolyU Database contains whole back surface of finger image as shown in figure. In order to concentrate only on the Finger knuckle

region in the FKP image, at first local co-ordinate system is constructed for each unprocessed image. Then Region of Interest (ROI) is extracted from the original image.

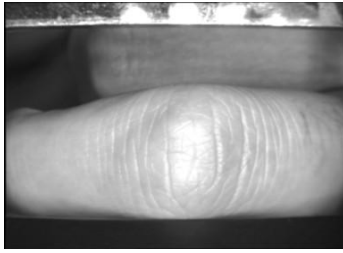


Figure 1 Input FKP Image

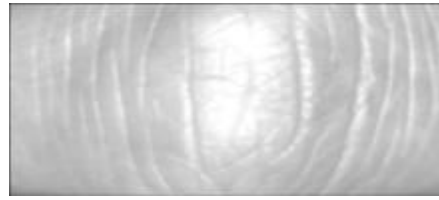


Figure 2 ROI Sub Image

2.2 Feature Extraction

C Hegde et al. [2] proposed the features extracted must be non-trivial and must not vary for a given person over time. We apply Gabor Wavelet transform on the image obtained after pre-processing. A Gabor wavelet is a complex planar wave restricted by a two dimensional Gaussian envelope. Gabor wavelet contains two components viz. real and imaginary. Aside from scale and orientation, the only thing that can make two Gabor wavelets differ is the ratio between wavelength and the width of the Gaussian envelope. Every Gabor wavelet has a certain wavelength and orientation, and can be convolved with an image to estimate the magnitude of local frequencies of that approximate wavelength and orientation in the image.



Figure 3 After edge Detection



Figure 4 After Dilating the edge

Walairach Nunsong et al. [4] proposed analysis of the FKP image, it is found that the following box sizes, 128×128 , 64×64 , 32×32 , 16×16 , 8×8 , and 4×4 occur the overcounting problem. In contrast, the undercounting problem occurs on box sizes 4×4 and 2×2 . It is evident that both problems occur on different box sizes. Therefore, the different problems should be solved by the different techniques. Based on this assumption, the box sizes are divided into three groups: (i) the first group is composed of the following box sizes, 128×128 , 64×64 , 32×32 , 16×16 , and 8×8 ; (ii) the second group is composed of only one box size, 4×4 ; and (iii) the last group is composed of only one box size, 2×2 .

In order to overcome the overcounting problem, a combination of the modified differential box-counting using weighted triangle-box partition and the improved triangle boxcounting methods or so-called CMI is applied to the first group. For the second group, both overcounting and undercounting problems occur on the box size 4×4 pixels. Thus, a discrimination constraint is necessary to use for classifying such problems.

2.2.1 Gabor Wavelet Filter

Farzam Kharaji et al. [5] described that the 2D Gabor function has been recognized as a very useful tool in feature extraction of image, due to its optimal localization properties in both spatial and frequency domain.

In addition to accurate time-frequency location, they also provide robustness against varying brightness and contrast of images. Furthermore, the filters can model the receptive fields of a simple cell in the primary visual cortex.

3. Feature Selection based on t-norms

Madasu Hanmandlu et al. [8] concatenated the features of all the FKP's resulting in a single feature vector. As we have a large number of features for the representation of FKP's, we are faced with the problem of dimensionality. To mitigate this problem of dimensionality, one can go in for the feature selection based on t-norms of divergence. Divergence: When the two features are used to represent the same pattern, the absolute difference between the features is termed as the divergence.

In the basic mode, Chetana Hegde, et al. [9] proposed the Radon Transform is applied on pre-processed FKP image and Eigen values are computed. Then they computed the correlation coefficient between the set of Eigen values stored in the database and that of input image to authenticate a person. For advanced level of security, Gabor Wavelet can be applied on pre-processed FKP image. The magnitude values of the Gabor Wavelet Transform are computed. Then the correlation coefficient between the set of magnitude values stored in the database and that of input image is used to authenticate a person. For real time implementation, suitable GUI can be developed. The basic mode of security system is found to have FAR as 6.79% and FRR as 0.0517%. The advanced mode has the FAR of about 3.07% and FRR as 1.14%.

3.1 Authentication

Chetana Hegde et al. [9] suggested authentication process involves a series of steps as listed here under.

1. The person who undergoes the authentication process should first enter his ID and his FKP image is captured.
2. The captured FKP image will undergo pre-processing techniques to get ROI and then to remove the possible noise and to increase the intensity.
3. Radon transform is applied on pre-processed FKP image to get a Radon image. Then Eigen values are calculated to get one feature set.
4. If one opts for basic mode of security, the correlation coefficient between the feature set retrieved from the database and newly computed feature set is calculated. If the value of correlation coefficient is greater than a threshold value 0:60, then the person can be authenticated. Otherwise he will be rejected.
5. If advanced mode is opted, then along with correlation coefficient between eigen values, the probability of successive match between Radon graph peaks is calculated.
6. Now, if both correlation coefficient and probability are greater than 0:60, the person is accepted, or else rejected.

4. Recognition Algorithms

Esther Rani P. et al. [10] developed that a bio metric system can recognize a person based on the algorithm built in to the system. These recognition algorithms are generally of two types 1) Identification algorithm which computes the template of the user and compares it with the templates stored in the database. It is also referred to as one to many matching. 2) Verification algorithm requires identity such as ID card, smart card or ID number for authentication.

The user template is then matched with the master template for recognition. It is also known as one to one matching. The verification algorithms must be accurate and identification algorithms must be accurate and very fast. The performance of a biometric system is based on the error rates. Two types of error rates are defined; False Acceptance Rate (FAR) and False Rejection Rate (FRR). They are defined as:

$$FAR = \frac{\text{Number of false acceptances}}{\text{Total number of imposter attempts}} \quad (1)$$

$$FRR = \frac{\text{Number of false rejections}}{\text{Total number of genuine attempts}} \quad (2)$$

The threshold value at which the FAR equals the FRR value is called the Equal Error Rate (EER). The accuracy of the biometric system is defined as:

$$\text{Accuracy} = \max (100 - (FRR+FAR)/2) \quad (3)$$

5. Threshold determination

Tao Kong et al. [11] described that the performance is affected by two parameters: δ and γ . Parameter δ can be defined as the corresponding matching score when FAR is equal to FRR, and parameter γ determines the number of users that Gabor cannot recognize successfully. So, the experimental performance will only be affected by the parameter γ . Let $\gamma = \delta \times \varepsilon$, and changing ε will lead to variation of γ . We will test the impact of parameter ε on the entire database. Table 1 lists the corresponding EER values of different ε .

Table 1 EERs (%) of different ε

ε	EER
0	1.230
0.02	0.753
0.04	0.382
0.06	0.244
0.08	0.218
0.10	0.265
0.12	0.369

6. Multi-algorithmic identification systems:

Abdallah Meraoumia et al. [12] described the integration of the two models. In their system, different fusion rules were tested to find the rule that optimizes the system accuracy. Thus, to find the better of the all rules, with the lowest EER, the *open set* and *closed set* identification have been set. For the *open set* identification, we can observe that all fusion rules improve the identification accuracy for all fingers. However, compared with the previous experiments (single algorithm), improvements in the LIF, LMF, RIF and RMF modality of approximately 34.000%, 47.000%, 32.500% and 32.300% are given. Thus, the test results shows that the LMF modality, with WHT rule, offers better results with a lower EER equal to 0.875% at a $T_o = 0.6862$.

The ROC curves provide a more detailed point of view of the performance of all multi algorithmic based *open set* identification systems. From the curves in this figure, it is clear to see the effectiveness of the LMF modality compared with the LIF, RIF and RMF modalities. Also, the efficiency of RIF modality is very clear. These results demonstrate that the proposed method is comparable with the previous FKP based identification approaches and other hand-based biometric technologies, including hand geometry, fingerprint and palmprint identification.

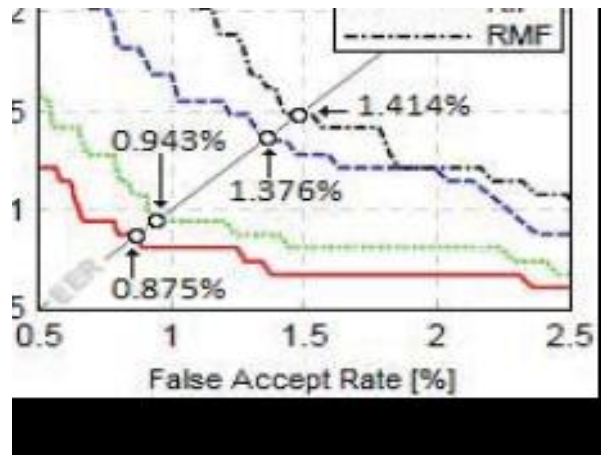


Figure 5 Multimodal identification test results The ROC curves under different types of finger.

7. Neural Net As Classifier

Karbhari V. Kale et al. [13] choose Multi-Layer Perceptron (MLP) with a back propagation learning algorithms for the proposed system. The MLP neural network has feedforward architecture within input layer, a hidden layer, and an output layer. During first stage of weights initialization some small random value are assigned. Each input unit receives the input signal x_i and forward towards hidden layer. Hidden layer sums its weighted input signals as,

$$y_{in} = b + \sum_{i=1}^n x_i v_{ij} \quad (4)$$

Where y_{in} is response of output unit, b is a bias, x_i is a input training vector and v_{ij} is a bias on hidden unit j . Relative activation function is

$$Z_j = f(y_{in}) \quad (5)$$

And it sends signals towards output layer. During the back propagation stage error is calculated as,

$$\delta_k = (t_k - y_k) f'(y_{in}) \quad (6)$$

Where t_k output target vector and y_k is output unit k . Each hidden unit sums its delta inputs from units in the layer above as.

$$\delta_{in} = \sum_{k=1}^m \delta_j w_{j k} \quad (7)$$

Where δ_j is error at hidden unit, w_{jk} is weights at hidden layer. Whereas error is calculated as,

$$\delta_j = \delta_{in} f'(y_{in}) \quad (8)$$

At the end each output unit updates its bias and weights as,

$$w_{new} = w_{old} + \Delta w_{ij}$$

$$b_{new} = b_{old} + \Delta b_{ij} \quad (9)$$

Where w_{new} , b_{new} are new weights and new bias w_{old} , b_{old} are old weights and old bias and Δw_{ij} and Δb_{ij} are weight correction and bias correction respectively. The stopping condition is error minimization.

8. Fusion

8.1 Image-Level Fusion Algorithm

Abdelhameed Ibrahim et al.[6] developed the goal of image fusion is to integrate multimodal, multiview, multisensor, multifocus, and multitemporal information into a new image containing information of which quality could not be achieved otherwise. A wide range of application areas utilizes image fusion. The fused image is suitable for the purposes of human/machine perception, and image processing tasks. This paper uses images of ear and FKs, which are collected from different sensors, and concatenate them side by side to get one image. The combined image then has all the features of ear and FKc images together.



Samples of Left Index



Right Index



Ear

8.2 Multi-Level Fusion Algorithm

Abdelhameed Ibrahim et al. [7] proposed a multi-level fusion algorithm at image level and classification level. First, we combine ear and FK (LI) images and extract the features of the combined image. Then, we classify these features using many classifiers (C1, C2, and C3) and combine the output of these classifiers in the abstract, rank, and score levels fusion (multi-level fusion). The outputs of nearest neighbor classifiers using majority voting is used in the abstract level, while the Borda count fusion method is used in the rank level.

8.3 Matching by vector consistency and fusion

Min-Ki Kim et al. [3] projected CIPs (Corresponding Interest points) into the same coordinate system, we can define direction vectors between each pair of CIPs. Let A and B be a pair of CIPs extracted from a reference image and a query image respectively. A direction vector V_i is defined as the directional line. If the FKP images are related by a translation, the direction vectors of each pair of CIPs will have similar direction and length. In practice, the variation in the FKP images is minimized by a capturing process and an ROI extraction process. Therefore the vector consistency can be used as a similarity measure between two FKP images. The similarity between two vectors V_1 and V_2 is defined as

$$S(V_1, V_2) = \frac{\min(l_1, l_2)}{\max(l_1, l_2)} \times \frac{180 - (|\theta_1 - \theta_2|)}{180} \quad (10)$$

where l_1 and l_2 are the lengths of V_1 and V_2 and θ_1 and θ_2 are the orientations of V_1 and V_2 . Therefore, the similarity score has the range from 0 to 1 and a value of 1 indicates identical length and orientation.

8.4 Comparison of fusion methods

Mohammed Saigaa et al. [14] suggested the measure of utility of a FKP system for a particular application can be described by two values. The False Acceptance Rate (FAR) is the ratio of the number of instances of pairs of different FKPs found to match to the total number of match attempts. The False Rejection Rate (FRR) is the ratio of the number of instances of pairs of the same FKP is found not to match to the total number of match attempts. FAR and FRR trade off against one another. That is, a system can usually be adjusted to vary these two results for a particular application, however decreasing one increase the other and vice versa.

The system threshold value is obtained based on the Equal Error Rate (EER) criteria where $FAR = FRR$. This is based on the rationale that both rates must be as low as possible for the biometric system to work effectively.

Another performance measurement is obtained from FAR and FRR which is called Genuine Acceptance Rate (GAR). It represents the identification rate of the system. In order to usually depict the performance of a biometric system, Receiver Operating Curves (ROC) are drawn. The ROC curve displays how the FAR changes with respect to the GAR and vice-versa. Biometric systems generate matching scores that represent how similar (or dissimilar) the input is compared to the stored template.

Table II A summary of fusion method

Method	Technique		Database size		Fusion level	EER	Recognition rate
			Class size	No of sample			
Fusion Method	Curvature based shape index	Multiple finger	86	8	Score level fusion		98
	PCS + LDA + ICA	Multiple finger	105	6	Score level fusion		98
	Gray level intensity + log-Gabor feature	Multiple finger	165	6	Feature level fusion		96.56
	Gray level intensity + log-Gabor feature	Multiple finger	165	6	Score level fusion		95.45
	2D-DFT	Palmprint and FKP	150	12	Score level fusion		
	Locality Preserving Projection	Palmprint and FKP	100	10	Score level fusion		99.56
	Directional coding and ridgelet transform	Palmprint and FKP	50	10	SVM based score fusion	.0034	

9. Conclusion:

Finger-Knuckle-Print is a unique & highly secure feature as a biometric identifier. Although Researchers have worked on this feature along with other biometric features, Its versatility nowadays make it popular among other as it can use inner or outer knuckle-print for ring, middle or other fingers. More work is yet to be done in this field. Use of various filters, wavelet transform and fusion with other biometric features enhance its uniqueness & accuracy.

10. References:

- [1] Swati M, RM. Ravishankar, "Finger Knuckle Print Recognition Based on Gabor feature and KPCA+LDA", Proceeding of International Conference on Emerging Trends in Communication, Control, Signal Processing and Computing Applications (C2SPCA), IEEE, Bangalore, India,(2013) October 10-11.
- [2] C Hegde, PD Shenoy, KR Venugopal, LM Patnaik, "FKP Biometrics for Human Authentication Using Gabor Wavelets", Proceeding of TENCON 2011, IEEE Region 10 Conference, (2011), pp. 1149-1153.
- [3] Min-Ki Kim, Patrick J. Flynn, "Finger-Knuckle-Print Verification Based on Vector Consistency of Corresponding Interest Points", IEEE Winter Conference on Applications of Computer Vision (WACV) – Steamboat Springs, CO, USA (2014.3.24-2014.3.26) IEEE Winter Conference on Applications of Computer Vision IEEE (2014), pp. 992-997.
- [4] Walairach Nunsong, Kuntpong Woraratpanya, "An Improved Finger-Knuckle-Print Recognition Using Fractal Dimension Based on Gabor Wavelet", 13th International Joint Conference on Computer Science and Software Engineering (JCSSE), IEEE, KhonKaen, Thailand, (2016) July 13-15.
- [5] Farzam Kharaji Nezhadian Saeid Rashidi, "Inner-knuckle-print for human authentication by using ring and middle fingers" ICSPIS 2016, Amirkabir University of Technology, Tehran, Iran, (2016) December 14-15, pp.1-6.
- [6] Abdel hameed Ibrahim, A. Tharwat, "Biometric Authentication Methods Based on Ear and Finger Knuckle Images", IJCSI International Journal of Computer Science Issues, vol. 11, issue 3, no. 1, (2014) May, pp. 134-138.
- [7] Madasu Hanm and lu, Jyotsana Grover, "Feature Selection for Finger Knuckle Print-based Multimodal Biometric System", International Journal of Computer Applications (0975 – 8887), vol. 38, no.10, (2012) January, pp. 27-33.
- [8] Chetana Hegde, P Deepa Shenoy, K R Venugopal, L M Patnaik, "FKP Biometrics for Human Authentication", TENCON 2011, IEEE Region 10 Conference- 2011 IEEE, Bali, Indonesia,(2011) November 21-24.
- [9] Chetana Hegde, Phanindra J, P Deepa Shenoy, L M Patnaik, "Human Authentication using Finger Knuckle Print", Proceeding COMPUTE '11 Proceedings of the Fourth Annual ACM Bangalore Conference Article No. 9, Bangalore, India, (2011) March 25 –26.
- [10] Esther Rani P, Shanmuga lakshmi R, "Finger Knuckle Print Recognition Techniques-A Survey", The International Journal of Engineering and Science (IJES), vol. 2, issue 11,(2013), pp. 62-69, ISSN (e): 2319–1813, ISSN (p): 2319 – 1805.
- [11] Tao Kong, Gongping Yang and Lu Yang Kong et al., "A hierarchical classification method for finger knuckle print recognition", EURASIP Journal on Advances in Signal Processing 2014, 2014:44 EURASIP Journal on Advances in Signal Processing, (2014), 2014:44.doi:10.1186/1687-6180-2014-44, pp.1-8.
- [12] Abdallah Meraoumia1, Salim Chitroub, Hakim Bendjenna and Ahmed Bouridane, "An Automated Finger-Knuckle-Print Identification System Using Jointly RBF & RFT Classifiers", (2016), 15th International Conference on Ubiquitous Computing and Communications and 2016 8th International Symposium on Cyberspace and Security, IEEE, DOI 10.1109/IUCC-CSS.2016.10, pp.17-22.
- [13] Karbhari V. Kale, Yogesh Rode, Majharoddin M. Kazi, Shrinivas Chavan, and Siddharth Dabhade, Prapti Deshmukh, "Multimodal Biometric System Using Finger Knuckle and Nail: A Neural Network Approach", International Journal of Electrical Energy, vol. 1, no. 4, (2013) December, pp. 222-227.
- [14] Mohammed Saigaa, Abdallah Meraoumia, Salim Chitroub and Ahmed Bouridane, "Efficient Person Recognition by Finger-Knuckle-Print Based on 2D Discrete Cosine Transform", International Conference on Information Technology and e-Services, IEEE, (2012), pp.1-6.